



Full paper



Self-powered control interface based on Gray code with hybrid triboelectric and photovoltaics energy harvesting for IoT smart home and access control applications

Chunkai Qiu^a, Fan Wu^a, Chengkuo Lee^b, Mehmet Rasit Yuce^{a,*}

^a Department of Electrical and Computer Systems Engineering, Monash University, Melbourne, VIC, 3800, Australia

^b Department of Electrical and Computer Engineering, National University of Singapore, 4 Engineering Drive 3, 117576, Singapore, Singapore

ARTICLE INFO

Keywords:

Triboelectric nanogenerator (TENG)
Self-powered
Hybrid energy harvesting
Smart home control
Authentication access control

ABSTRACT

The rapid expansion of Internet of Things (IoT) in many living environments, such as smart home, has motivated the development of human-machine interfaces (HMIs) for the interactions between human and machine. In this paper, a sliding operation triboelectric nanogenerator (TENG) based control disk interface, generating 3-bit binary-reflected Gray-code (BRGC), is developed by integrating copper electrodes, polytetrafluoroethylene (PTFE) film, photovoltaic cell, and electronic signal processing circuits. Eight sensing transitions are successfully achieved by the 3-bit BRGC encoding patterns with two electrodes. One electrode represents the binary bit "0"; another electrode represents the binary bit "1". A third electrode located in the middle of the disk is utilized to indicate the sliding directions (inward or outward). The output signal detection mechanism and signal processing circuit have been developed, and a Bluetooth transmitter is employed for enabling controlling applications wirelessly. Besides the self-powered sensing characteristic of the triboelectric control disk, a hybrid energy harvester that can harvest triboelectric and photovoltaics energy is proposed to power the entire electronic control circuit. Finally, this triboelectric control disk is employed as a self-powered interface for smart home control and password authentication access control system, which exhibits promising reliability, practicality, and flexibility.

1. Introduction

Internet of Things (IoT) has become a promising technological paradigm and is rapidly gaining various research interests in recent years [1–5]. According to Ref. [3], it is predicted that there will be 26 to 50 billion Internet-connected devices by 2020 and 100 billion devices by 2030. These devices will be deployed in different environments, such as traffic, health, logistic, retail, agriculture, smart cities, smart grids, and smart homes, to perform sensing, identifying, networking, and computation [4]. Among these IoT domains, there is increasing research attention in smart homes over the past few years [5]. In a typical smart home domain, household devices are equipped with wireless communication interface, forming a home-based wireless sensor network (WSN), where the sensed data from the devices are forwarded to and computed at a central station that is called as home sink or home hub [5].

Among many commercially available smart home applications,

besides autonomous turning lights or appliances on and off according to the surrounding environments, such as light intensity, relative humidity, and temperature, or a user pre-configured protocol, lights and devices can also be controlled by mechanical switches. However, mechanical switches have limited scalability because one mechanical switch can only control one appliance. This may result in the requirement of a substantial amount of mechanical switches in a house. Furthermore, mechanical switches have a limited lifetime and finite flexibility. Human-machine interfaces (HMIs) play an essential role in IoT applications to operate different Internet-connected objects, which can help to exchange information between humans and electric devices effectively [6–10]. Therefore, designing an intelligent and smart control interface for smart objects is of great importance.

In the last few years, thanks to the invention of triboelectric nanogenerator (TENG) by Prof. Z. L. Wang's group [11–14], more creative and intelligent sensing methods have been designed and developed using TENG. TENG is based on the electrification and electrostatic

* Corresponding author.

E-mail address: mehmet.yuce@monash.edu (M.R. Yuce).

induction effects, which can act as a self-powered sensor to detect human interaction and provide useful information for controlling different objects by converting a mechanical triggering into a self-generated electric signal [15–23]. The signal can be processed and analyzed further by a microcontroller (MCU) or a computer to provide useful information as active sensors. TENG can be easily applied in the conventional keyboard to realize HMI [19,24]. For instance, a TENG-based intelligent keyboard is proposed for keystroke dynamics investigation and energy harvesting purposes [25], and a TENG-array which can detect keystroke dynamics is used to achieve authentication and identification in Ref. [26]. TENG based sensors can also be applied to detect human motion. For example, work [6] presents a TENG glove-based control interface that can detect finger movements for diverse control applications, such as a remote control drone and vehicle. TENG can also be applied as flexible tactile sensors for electronic skin. For instance, a stretchable, transparent and self-healing ionic-skin for powering electronics devices is presented in Ref. [27], and work [28] proposes another self-powered electronic skin for actively detecting human motions and environmental atmosphere.

In addition to the numerous applications in self-powered sensors, TENG has demonstrated great potential in energy harvesting systems. The TENG can be applied to harvest different mechanical energy in our daily life, such as human motion [29–31], vibration [32–34], air flow [35–38], water wave [39–42], and acoustic [43–45]. The triboelectric induced energy can be stored in an energy storage that is typically a supercapacitor and then the stored energy can be utilize to power some other electronic devices [46–49].

Herein, this paper presents an innovative self-powered TENG-based control disk interface for IoT smart home and access control applications. The sensor interface is developed based on binary coding mechanism, which utilizes two sensing electrodes. One electrode represents the binary bit “0”, while the other one represents the binary bit “1”. Furthermore, by introducing an additional electrode in the middle position of the control disk, sliding directions across the electrodes can be

obtained. With the binary coding mechanism, multiple sensing patterns can be identified by sliding finger across the electrodes, which can be applied for different applications. Moreover, the sliding speed can be derived from the output signals and used as a control signal. Apart from controlling functionalities, the TENG-based sensor is integrated with a small-sized photovoltaic cell forming a hybrid energy harvester, which is able to scavenge both light and triboelectric energy in order to provide sufficient power for the entire electronic circuit. A Bluetooth Low Energy (BLE) based MCU is utilized to recognize and decode the output signals from the sensor and also transmit real-time control signals to different appliances. The TENG control disk exhibits exceptional advantages over mechanical switches, including self-powered, portable, multi-functional, high reliability and scalability, low-cost, and easy fabrication. In comparison with other reported TENG-based HMIs, the proposed control interface offers higher robustness in coding and identification, and admirable practicality due to the compact size of the device and self-powered electronic circuits. The proposed control disk interface has been tested in different applications, including the smart home appliances control and the door access authentication control, which demonstrates promising potentials as a new control interface for human-machine interactions in IoT applications.

2. System design and working mechanism

The structure of the proposed self-powered TENG control disk interface is illustrated in Fig. 1(a). The control disk mainly consists of a standard two-layer printed circuit board (PCB) and a polytetrafluoroethylene (PTFE) film overlay which serves as a friction contact surface. The thickness of the copper (Cu) layer of the PCB is approximately 35 μm . The control disk includes two patterned Cu sensing electrodes (E-1 and E-2) based on 3-bit binary-reflected Gray-code (BRGC) to form a patterned control array. The patterned Cu electrodes are printed on the top layer of PCB. E-1 is utilized to represent binary bit “1” in BRGC, and E-2 represents binary bit “0” in BRGC. E-2 consists of two pieces of Cu

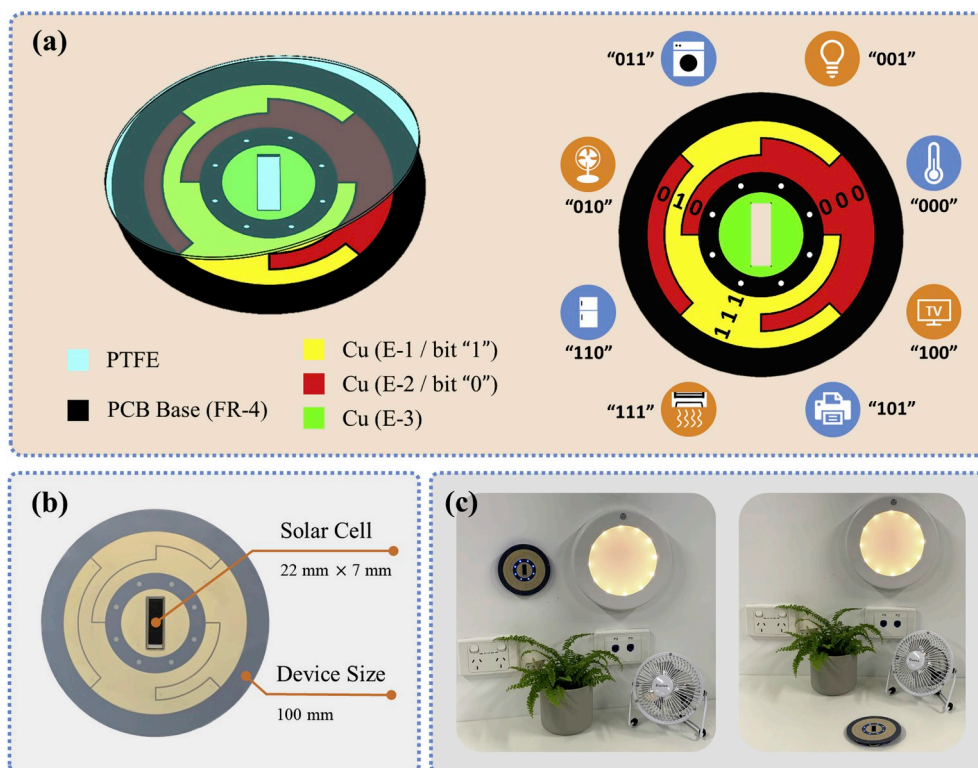


Fig. 1. System overview of the self-powered TENG control disk. (a) Structure layout of the TENG control disk. (b) Dimensions of the device. (c) Photographs of the TENG device. The device can be attached to the wall or the desk to control smart appliances wirelessly.

electrodes which are connected through the connection wires on the bottom layer of PCB. With 3-bit BRGC, eight sensing patterns can be realized. Besides the two essential BRGC patterned sensing electrodes (E-1 and E-2), one additional electrode (E-3) is used for detecting the sliding direction across the patterned electrodes, i.e., sliding inwards or outwards (sliding inwards: from the edge to the center; sliding outwards: from the center to the edge). The sliding direction is a control signal which can be used to turn a specific appliance on or off. A BRGC starts with a voltage peak generated on E-3, which indicates that the sliding gesture is from the center to the edge. Followed by a BRGC ended with a voltage peak generated on E-3, this means the sliding gesture is from the edge to the center. Fig. 1(b) and (c) show a developed self-powered control disk. The control disk has a dimension of 100 mm. More detailed dimensions of the control disk are provided in Fig. S1 (Supporting Information). A solar cell with a size of 22 mm × 7 mm is integrated with the TENG control disk to achieve hybrid solar and triboelectric energy harvesting. The energy can be used to power the electronic circuits and BLE module for smart home control purpose. The compact size of the device enables it to be attached to the wall or the desk for wireless controlling applications.

The working mechanism of the proposed control disk is systematically illustrated in Fig. 2. At the beginning, a finger (with nitrile glove) contacts with the PTFE film surface, as shown in Fig. 2(a, i). Because of

the significant difference in electron-attracting ability, the electrons will be attracted by the PTFE film from the nitrile glove surface, which results in a positively charged finger surface and a negatively charged PTFE surface. The charges will remain on the surface for a long time. Accordingly, the negative charges on the PTFE surface will induce positive charges on Cu electrode due to triboelectric induction effect. When the finger begins to slide across the electrode as depicted in Fig. 2 (a, ii), the positive charges on the finger will drive electrons flow to the Cu electrode from the ground due to the triboelectric induction. The net amount of positive charges on the electrode reduces and an electric current is generated in the load until a new electric potential equilibrium is reached, as shown in Fig. 2(a, iii). As the finger moves away from the electrode, electrons flow back to the ground, generating a negative current in the load and the Cu electrode becomes positively charged again as illustrated in Fig. 2(a, iv). Therefore, an alternating electric signal is generated as a consequence of sliding across the electrode. Based on this working mechanism, a TENG coding principle is developed.

Fig. 2(b) and (c) depict the coding principle of the TENG control disk to turn on and turn off a smart appliance, respectively. The coding pattern “001” is used as an example here. The gesture that is used to turn on appliances is to slide outwards across the patterned electrodes. As the finger touches E-3 and slides outwards from the center of the

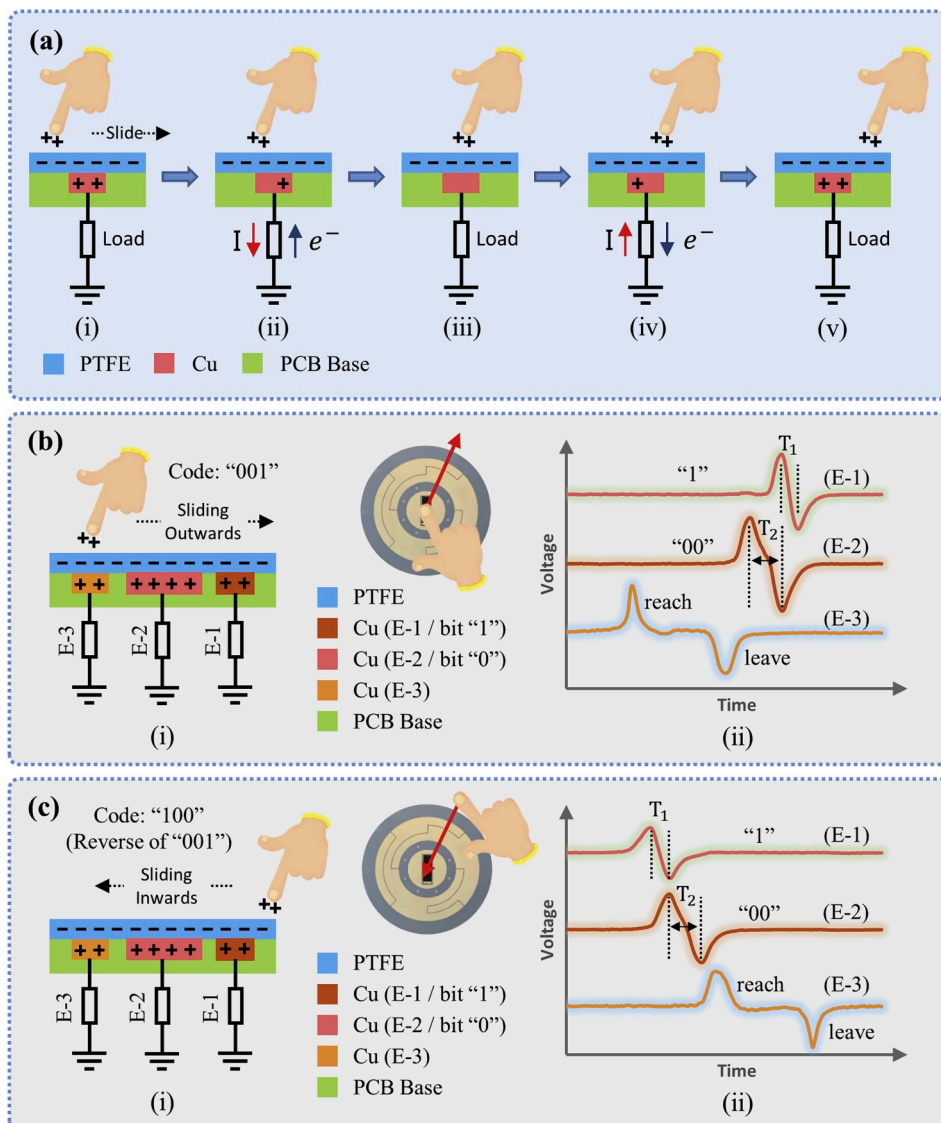


Fig. 2. Operation principle of the TENG control disk. (a) The working mechanism of the output signal generating processes based on sliding operation across the individual sensing electrode. (b) The coding principle and output signals of the device when the finger is sliding outwards across the patterned electrodes “001”, which can be used as the control signal to turn on a smart appliance. (c) The coding principle and output signals of the device when the finger is sliding inwards across the patterned electrodes “001”, which can be used as the control signal to turn off a smart appliance. Since the sliding direction is reversed, the code “100” which is the reverse of code “001”, is detected at the output.

control disk and across the patterned electrodes, three output voltage peaks are generated on three electrodes respectively, as shown in Fig. 2 (b, ii). The output voltage peak on E-1 represents the BRGC binary bit “1”, and the output voltage peak on E-2 represents the BRGC binary bit “0”. The relative width of the electrodes indicates the number of binary bits in the code. Therefore, for the coding pattern “001”, the physical width of E-2 is twice the size of E-1. A wider electrode will produce a wider signal pulse, because the relatively longer time is required to slide across the electrode. Due to the relative width of E-1 and E-2, the pulse width T2 is two times larger than the pulse width T1, as shown in Fig. 2 (b, ii). The crest and trough of the pulse waves are selected as the indication of the pulse width, since these two points can be identified easily. Therefore, from the output pulse width T1 and T2, the device can recognize there are two bits “0” and one bit “1” in the code. Moreover, the pulse on E-2 is generated before the pulse on E-1, which indicates that two bits “0” are followed by one bit “1” in the code. From the relative pulse width (T1 and T2) and the timestamp of the pulses, the code “001” can be recognized. Besides, as the finger reaches and leaves E-3, a positive voltage peak and a negative voltage peak are generated correspondingly. Hence, from the timestamp of the signal pulses, direction sensing can be realised as well. In this example, the pulse on E-3 is generated before the code pulses “001”, which indicates the sliding direction is from the center of the device to the edge. In contrast, as shown in Fig. 2(c), the pulse generated on E-3 is after the code pulses “100”, which indicates a reverse sliding direction (sliding inwards). In this way, an appliance can be turned on if the sliding direction is outward, and turned off if slide inwards. The decoding mechanism and output signals of “000” and “010” are illustrated in Fig. S2 and Fig. S3 respectively in Supporting Information. The summary of the codes triggered by sliding outwards and inwards across the eight sensing patterns is provided in Fig. S4 (Supporting Information). A video demonstration showing the operation of the TENG control disk can be found in Video S1 (Supporting Information).

Supplementary video related to this article can be found at <https://doi.org/10.1016/j.nanoen.2020.104456>.

The effect of the sliding speeds on the output signals has been investigated, as illustrated in Fig. 3. Fig. 3(a)–(c) demonstrate the performance of the output when sliding with slow (~60 mm/s), normal (~100 mm/s), and fast (~200 mm/s) speeds across the coding pattern “001” at a frequency of 1 Hz, respectively. The peak of the output voltage signal increases with the higher sliding speed from 10 V at slow sliding speed to 40 V at fast sliding speed. Although the time intervals T1 and T2 decrease with the higher sliding speed, the time ratio of T2 over T1, which represents the number of bits “0” and “1” in the code, is almost identical ($T2/T1 \sim 2$) regardless of various sliding speeds. The average time ratio of T1 and T2 ($T2/T1$) is 1.85, 1.70, and 1.72 at slow, normal, and fast sliding speeds, respectively. The consistent time interval ratio under various sliding speeds shows the robustness of the coding mechanism. The result reveals that the TENG control disk is able

to function under various sliding speeds with accurate coding recognition. Furthermore, different levels of sliding speeds can be derived from the output time intervals. Therefore, the sliding speed can be used as a control signal as well, e.g., to control the brightness level of lights or the speed setting of fans.

3. Hybrid energy harvesting

A hybrid energy harvester is proposed to harvest both TENG and solar energy in order to power the electronic circuits of the sensor interface. The TENG can generate electricity from mechanical impact, e.g., hand tapping. In the meantime, the solar cell can scavenge energy from natural and artificial light sources. The hybrid energy generated from TENG and solar cell can be stored either in a supercapacitor or in a rechargeable battery to power the electronic circuits. To verify the energy harvesting capability of the proposed TENG, the electric outputs from hand tapping have been investigated, as shown in Fig. 4(a)–(e). All of the three electrodes (E-1, E-2, and E-3) are connected together to the load to maximize the output power. Fig. 4(b) and (c) depict the open-circuit voltage (measure by a 100 Mohm probe) and short-circuit current of the TENG under repeated hand tapping with a frequency about 3 Hz. The average peak open-circuit voltage (V_{oc}) is about 570 V, and the average peak short-circuit current (I_{sc}) is about 30 μ A. With every hand tapping, the amount of induced charges is about 210 nC, as shown in Fig. 4(d). The quantity of charges induced by hand tapping is obtained by integrating the short-circuit current $I_{sc} - t$ curve. Fig. 4(e) demonstrates the charging curve of a 10 μ F capacitor which is charged by the TENG disk under hand tapping via a full-wave rectifier. The capacitor is charged from 0 V to 4.8 V in 60 s via the hand tapping at a frequency of 3 Hz. In Fig. 4(f), the charging curves of a 0.33 F supercapacitor which is charged by the solar cell under natural sunlight and artificial light sources are illustrated. The photovoltaic cells power management chip ADP5090 is utilized to store the power generated by the solar cell to the supercapacitor. During the experiment, the solar panel is exposed to the sun at the irradiance level of 1000 W/m². The supercapacitor is charged from 2 V to 3 V in 100 s. On the other hand, when the solar cell is illuminated at a distance of 30 cm under a 40 W table lamp in which the irradiance level is 400 W/m², the supercapacitor can be charged from 2 V to 3 V in 230 s. The TENG energy harvester and solar cell energy harvester are connected in parallel to store the energy in a rechargeable battery. The hybrid energy harvesting circuit is shown in Fig. S5 (Supporting Information). The stored energy is used as a power source to function the entire electronic circuit of the control disk, which is sufficient for both indoor and outdoor applications.

4. Application 1: smart home control

A smart home control system is developed based on the proposed

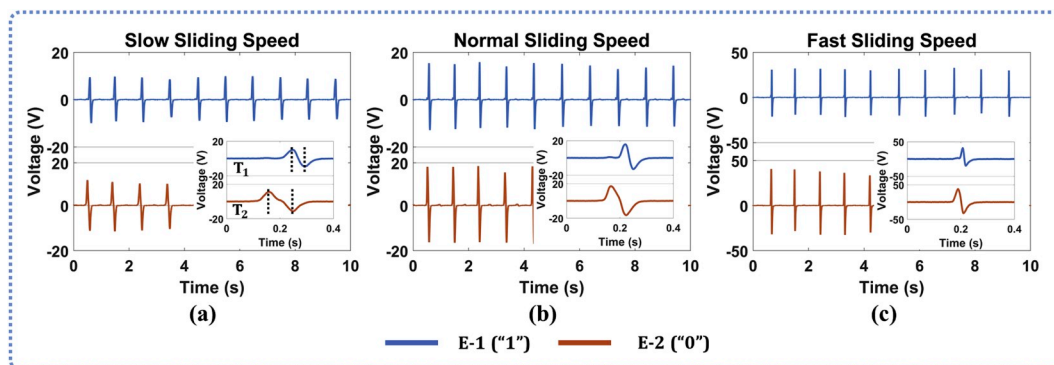


Fig. 3. The output voltage of the patterned electrodes (“001” as the example here) under different sliding speeds: (a) slow (~60 mm/s), (b) normal (~100 mm/s), and (c) fast (~200 mm/s).

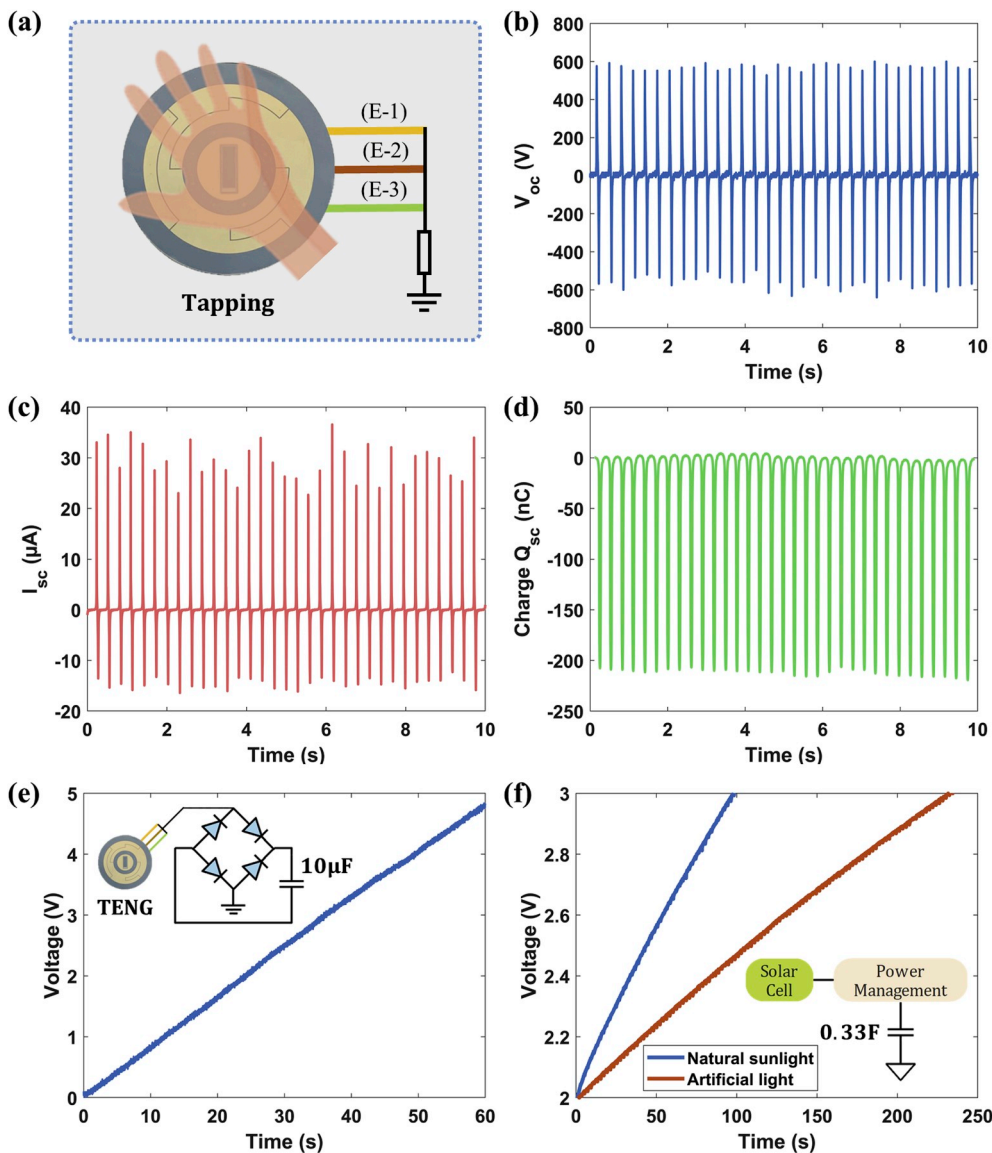


Fig. 4. Hybrid energy harvesting with the TENG control disk and the photovoltaic cell. (a) The illustration of the TENG device under hand tapping. (b) The open-circuit voltage of the TENG device under hand tapping. (c) The short-circuit current of the TENG device under hand tapping. (d) The amount of induced charges when the device is under hand tapping. (e) A $10 \mu\text{F}$ capacitor is charged by the TENG device under hand tapping. (f) The charging curves of a 0.33 F supercapacitor with the photovoltaic cell under natural sunlight and artificial light.

TENG control disk, as demonstrated in Fig. 5. Fig. 5(a) depicts the structure of the TENG control device. The front side of the device is the TENG sensor, and the back side of the device is the electronic circuits, including signal processing circuit, power management circuit, and a rechargeable battery to store the hybrid energy scavenged by TENG and solar cell. The detailed structure layout of the fabricated device is shown in Fig. S6 (Supporting Information). A MCU with BLE 5.0 module (MDBT42Q) is employed to achieve wireless smart appliances control. The block diagram of the entire smart home control system is illustrated in Fig. 5(b). As the finger sliding across the patterned electrodes, the output voltage signals generated by the TENG control disk are detected and processed by the signal processing circuit and MCU. When different codes are detected, corresponding instructions will be sent via a BLE network to control the smart appliances. Fig. 5(c) presents four examples of TENG electric signals corresponding to the sliding motion to turn on different appliances in the home. The electric signals corresponding to the sliding motion to turn off smart appliances is shown in Fig. 5(d). The output signals of all the eight sensing patterns are depicted in Fig. S7 and Fig. S8 (Supporting Information). Furthermore, different levels of sliding speeds can be derived from the time intervals of signal pulse, as depicted in Fig. 5(e). Therefore, the sliding speeds can be used as a signal to control the brightness level of lights or the speed setting of fans. The

photographs showing three brightness levels of a light controlled by the TENG device are shown in Fig. S9 (Supporting Information). The power consumption of the device is 18 mA at 3.3 V power supply when it is activated for sensing and wireless controlling. For each controlling operation, the energy consumption of the device can be recovered in 55 s by solar energy harvester, as illustrated in Fig. S10 (Supporting Information). Moreover, to reduce the power consumption of the control device, the system is programmed to go into a sleep mode after 5 s idle state. The power consumption of the device is $0.3 \mu\text{A}$ at 3.3 V power supply in the sleep mode. Despite the electronic control circuit is mainly powered by the photovoltaic cell, the TENG has shown promising advantages as an additional power source. As illustrated in Fig. S11 (Supporting Information), the TENG can be used to recover the energy consumption of the device that is in sleep mode. The energy consumption of the device in sleep mode for 120 s can be recovered by tapping the TENG in about 40 s . Assuming the control device is required to operate every 20 min and each operation requires 10 s , the average power consumption of the device is about 0.5 mW . The system can be waked up from the sleep mode by tapping on the sensor. The tapping motion generates a voltage peak on E-3 that is used to wake up the system from the sleep mode. A video demonstration of the real-time smart home control can be found in Video S2 (Supporting Information).

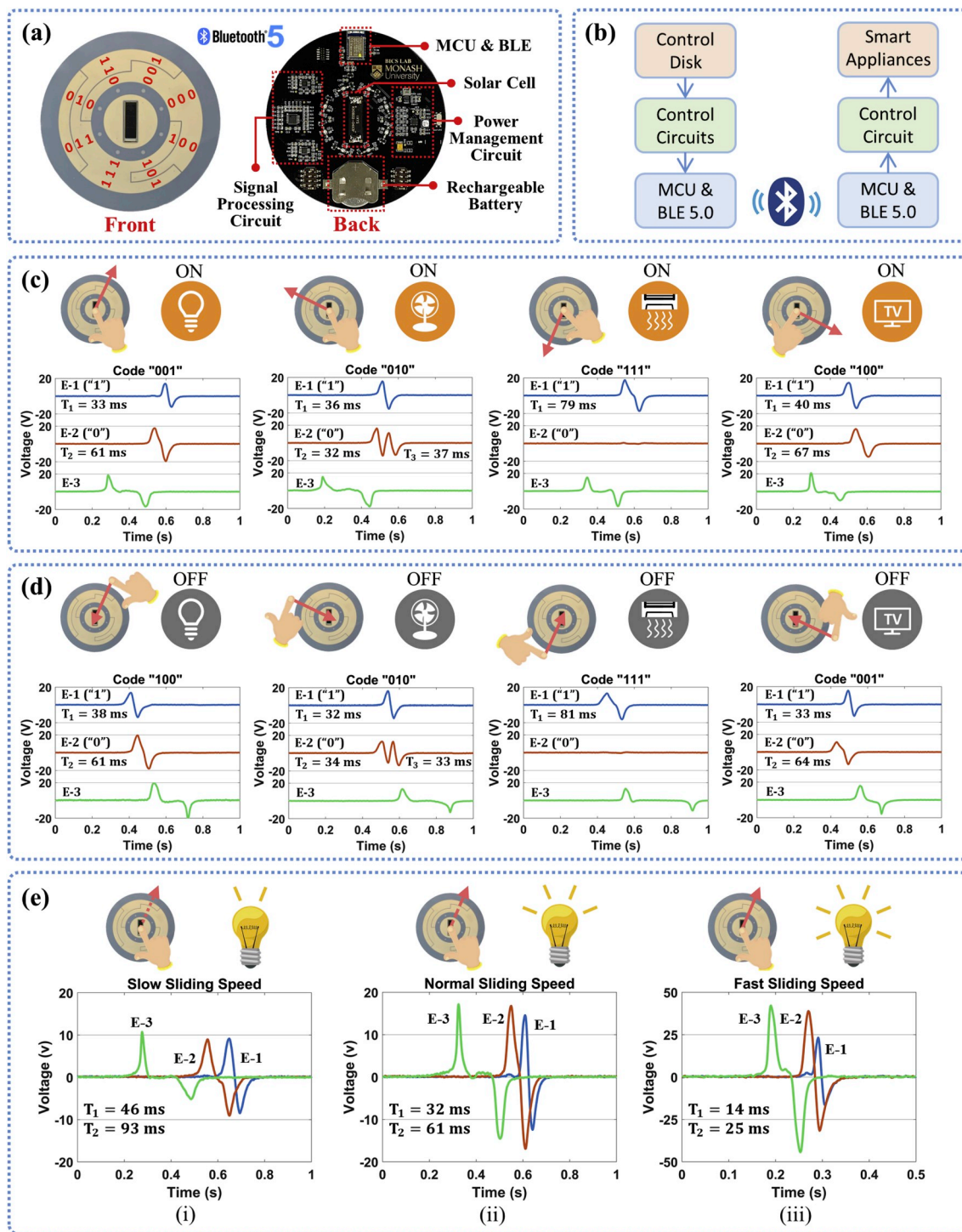


Fig. 5. Smart home control with the TENG control disk. (a) The front and back view of the self-powered TENG device. (b) Block diagram of the wireless smart home control system. (c) Four examples showing the output signals corresponding to the sliding operation to turn on four smart appliances. (d) Four examples showing the output signals corresponding to the sliding operation to turn off four smart appliances. (e) Demonstration of using various sliding speeds to control the brightness of the light.

Supplementary video related to this article can be found at <https://doi.org/10.1016/j.nanoen.2020.104456>.

5. Application 2: home authentication access control system

The TENG control disk can also provide a solution for self-powered password authentication entry system. A flexible, efficient, and secure smart home entry system has been developed, as shown in Fig. 6(a).

With 3-bit BRGC coding, 8 digits (0–7) can be realised. The door access can be obtained by entering a 6-digit entry password. There are more than 262,000 combinations of potential passwords based on this configuration, which is sufficient for everyday needs. Fig. 6(b) illustrates the block diagrams of two separate modules of the smart home entry system. The outdoor module consists of the TENG control disk, TENG control circuits, and a MCU for digits decoding; the indoor module mainly includes the MCU for password recognition and a control circuit

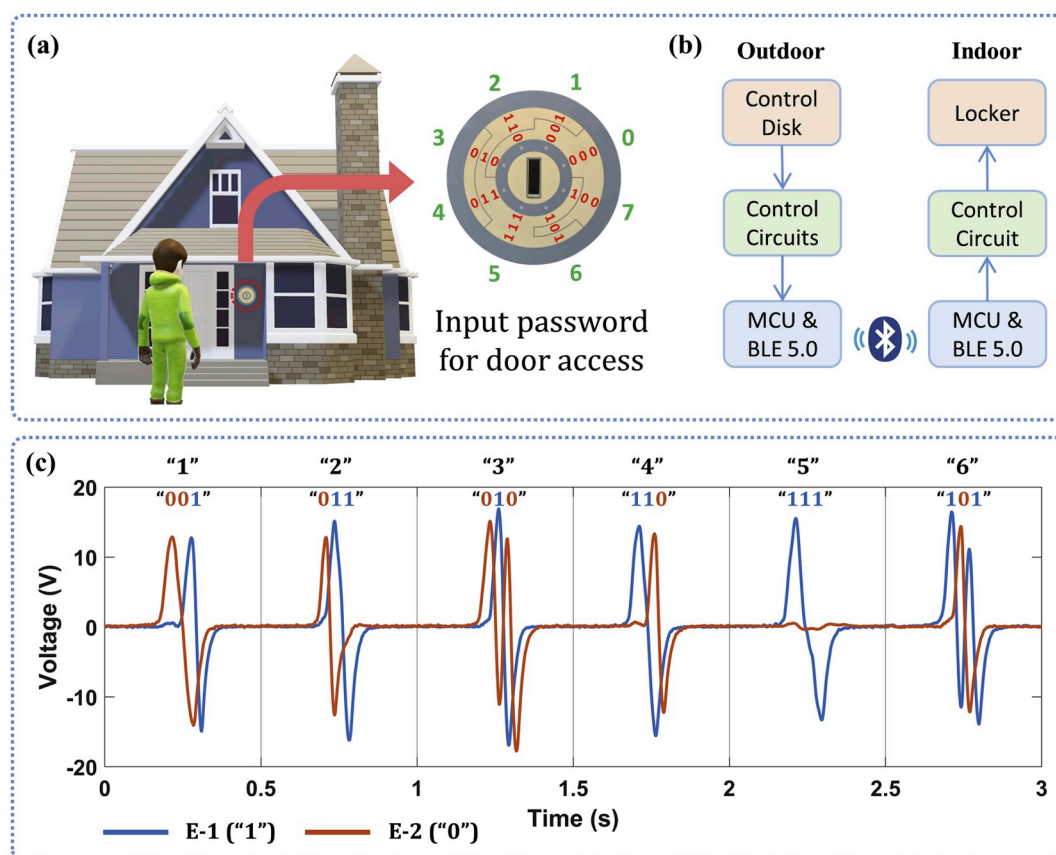


Fig. 6. Authentication access control by using the self-powered TENG control disk. (a) The illustration of the password authentication access control system. A password is required to enter the door. (b) Block diagram of the access control system. (c) Demonstration of the output signals when the password “123456” is entered.

for the door locker. In daily operation, after the outdoor module is waked up by the homeowner via hand tapping from the sleep mode to input password, the MCU will start to decode the corresponding output signal generated by the TENG control disk. The outdoor module will transmit the decoded digits to the indoor module through the BLE network. If the 6-digit password (“123456”) has been entered, the door will be opened. Fig. 6(c) depicts an example output signal of the password “123456”. Since only the outward sliding operation is needed for password entering, only 2 electrodes (E-1 and E-2) are required here. The third electrode (E-3) may be used for direction sensing (sliding outward or inward) if needed. Hence, 16 digits can be realised from the TENG control disk, which will further improve the numbers of combinations of potential passwords (a total of 16,777,216 potential 6-digit password combinations). A small door model is designed and built for the demonstration purpose as shown in the Supporting Information Fig. S12. A video demonstration of the real-time home authentication entry system can be found in Video S3 (Supporting Information).

Supplementary video related to this article can be found at <https://doi.org/10.1016/j.nanoen.2020.104456>.

6. Conclusion

In this paper, an innovative self-powered triboelectric control disk interface is proposed for IoT smart home control and authentication access control applications. Based on the binary coding mechanism, by using only two sensing electrodes (one serves as binary bit “1”; the other serves as binary bit “0”), multiple sensing transitions can be achieved. An additional electrode can be employed to indicate the sliding directions across the patterned electrodes. Eight codes can be encoded on the sensor through 3-bit binary code to achieve eight control

instructions, leading to sufficient number of codes and control signals for controlling of devices in a home environment. Furthermore, a hybrid energy harvester, which incorporates the proposed TENG control interface and solar cell, is designed to scavenge both the mechanical energy from hand tapping and the energy of light to power the electronic circuits. A smart home control system has been developed and demonstrated the feasibility of utilizing the TENG control disk as a HMI. The system can detect the output signal of the control disk accurately and then send the corresponding commands to control the smart appliances in real-time via a BLE network, such as to turn on or turn off the light and the fan. With slow to fast sliding speeds across the electrodes, the brightness of the light will be adjusted from minimum to maximum level accordingly. In addition, the control disk can be used as a password input interface as well. An authentication access control system is demonstrated by inputting password to gain the door access. The self-powered, multi-functional, and portable TENG control disk with high scalability and reliability exhibits significant advantages in IoT enabled devices controlling, such as smart home, smart building, and remote robotics control.

Declaration of competing interest

The authors declare that they have no known competing financial interests or personal relationships that could have appeared to influence the work reported in this paper.

Acknowledgment

M. R. Yuce’s work has been supported by Australian Research Council Future Fellowships Grant (FT130100430).

Appendix A. Supplementary data

Supplementary data to this article can be found online at <https://doi.org/10.1016/j.nanoen.2020.104456>.

References

- [1] L. Atzori, A. Iera, G. Morabito, The Internet of Things: a survey, *Comput. Network.* 54 (2010) 2787–2805.
- [2] A. Whitmore, A. Agarwal, L. Da Xu, The Internet of Things – a survey of topics and trends, *Inf. Syst. Front.* 17 (2015) 261–274.
- [3] E.A. Rogers, E. Junga, Intelligent Efficiency Technology and Market Assessment, American Council for an Energy-Efficient Economy (ACEEE), 2017.
- [4] A. Colaković, M. Hadzialić, Internet of Things (IoT): a review of enabling technologies, challenges, and open research issues, *Comput. Network.* 144 (2018) 17–39.
- [5] B.L.R. Stojkoska, K.V. Trivodaliev, A review of Internet of Things for smart home: challenges and solutions, *J. Clean. Prod.* 140 (2017) 1454–1464.
- [6] T. He, Z. Sun, Q. Shi, M. Zhu, D.V. Anaya, M. Xu, T. Chen, M.R. Yuce, A.V.-Y. Thean, C. Lee, Self-powered glove-based intuitive interface for diversified control applications in real/cyber space, *Nano Energy* 58 (2019) 641–651.
- [7] Q. Shi, C. Qiu, T. He, F. Wu, M. Zhu, J.A. Dziuban, R. Walczak, M.R. Yuce, C. Lee, Triboelectric single-electrode-output control interface using patterned grid electrode, *Nano Energy* 60 (2019) 545–556.
- [8] S. Lim, D. Son, J. Kim, Y.B. Lee, J.-K. Song, S. Choi, D.J. Lee, J.H. Kim, M. Lee, T. Hyeon, et al., Transparent and stretchable interactive human machine interface based on patterned graphene heterostructures, *Adv. Funct. Mater.* 25 (2015) 375–383.
- [9] X. Pu, H. Guo, J. Chen, X. Wang, Y. Xi, C. Hu, Z.L. Wang, Eye motion triggered self-powered mechno sensational communication system using triboelectric nanogenerator, *Sci. Adv.* 3 (2017).
- [10] B. Zhang, Y. Tang, R. Dai, H. Wang, X. Sun, C. Qin, Z. Pan, E. Liang, Y. Mao, Breath-based human-machine interaction system using triboelectric nanogenerator, *Nano Energy* 64 (2019) 103953.
- [11] F.-R. Fan, Z.-Q. Tian, Z.L. Wang, Flexible triboelectric generator, *Nano Energy* 1 (2012) 328–334.
- [12] Z.L. Wang, Triboelectric nanogenerators as new energy technology for self-powered systems and as active mechanical and chemical sensors, *ACS Nano* 7 (2013) 9533–9557.
- [13] T. Jiang, L.M. Zhang, X. Chen, C.B. Han, W. Tang, C. Zhang, L. Xu, Z.L. Wang, Structural optimization of triboelectric nanogenerator for harvesting water wave energy, *ACS Nano* 9 (2015) 12562–12572.
- [14] C. Zhang, W. Tang, C. Han, F. Fan, Z.L. Wang, Theoretical comparison, equivalent transformation, and conjunction operations of electromagnetic induction generator and triboelectric nanogenerator for harvesting mechanical energy, *Adv. Mater.* 26 (2014) 3580–3591.
- [15] S. Niu, Z.L. Wang, Theoretical systems of triboelectric nanogenerators, *Nano Energy* 14 (2015) 161–192.
- [16] Z.L. Wang, Triboelectric nanogenerators as new energy technology and self-powered sensors—principles, problems and perspectives, *Faraday Discuss* 176 (2015) 447–458.
- [17] S. Wang, L. Lin, Z.L. Wang, Triboelectric nanogenerators as self-powered active sensors, *Nano Energy* 11 (2015) 436–462.
- [18] X. He, Y. Zi, H. Yu, S.L. Zhang, J. Wang, W. Ding, H. Zou, W. Zhang, C. Lu, Z. L. Wang, An ultrathin paper-based self-powered system for portable electronics and wireless human-machine interaction, *Nano Energy* 39 (2017) 328–336.
- [19] W. Ding, A.C. Wang, C. Wu, H. Guo, Z.L. Wang, Human-machine interfacing enabled by triboelectric nanogenerators and tribotronics, *Adv. Mater. Technol.* 4 (2019) 1800487.
- [20] X. Pu, H. Guo, Q. Tang, J. Chen, L. Feng, G. Liu, X. Wang, Y. Xi, C. Hu, Z.L. Wang, Rotation sensing and gesture control of a robot joint via triboelectric quantization sensor, *Nano Energy* 54 (2018) 453–460.
- [21] J. Chen, W. Xuan, P. Zhao, U. Farooq, P. Ding, W. Yin, H. Jin, X. Wang, Y. Fu, S. Dong, J. Luo, Triboelectric effect based instantaneous self-powered wireless sensing with self-determined identity, *Nano Energy* 51 (2018) 1–9.
- [22] Q. He, Y. Wu, Z. Feng, C. Sun, W. Fan, Z. Zhou, K. Meng, E. Fan, J. Yang, Triboelectric vibration sensor for a human-machine interface built on ubiquitous surfaces, *Nano Energy* 59 (2019) 689–696.
- [23] Z. Lin, J. Yang, X. Li, Y. Wu, W. Wei, J. Liu, J. Chen, J. Yang, Large-scale and washable smart textiles based on triboelectric nanogenerator arrays for self-powered sleeping monitoring, *Adv. Funct. Mater.* 28 (2018) 1704112.
- [24] W. Yin, Y. Xie, J. Long, P. Zhao, J. Chen, J. Luo, X. Wang, S. Dong, A self-power-transmission and non-contact-reception keyboard based on a novel resonant triboelectric nanogenerator (r-teng), *Nano Energy* 50 (2018) 16–24.
- [25] J. Chen, G. Zhu, J. Yang, Q. Jing, P. Bai, W. Yang, X. Qi, Y. Su, Z.L. Wang, Personalized keystroke dynamics for self-powered human-machine interfacing, *ACS Nano* 9 (2015) 105–116.
- [26] C. Wu, W. Ding, R. Liu, J. Wang, A.C. Wang, J. Wang, S. Li, Y. Zi, Z.L. Wang, Keystroke dynamics enabled authentication and identification using triboelectric nanogenerator array, *Mater. Today* 21 (2018) 216–222.
- [27] K. Parida, V. Kumar, W. Jiangxin, V. Bhavanasi, R. Bendi, P.S. Lee, Highly transparent, stretchable, and self-healing ionic-skin triboelectric nanogenerators for energy harvesting and touch applications, *Adv. Mater.* 29 (2017) 1702181.
- [28] Y. Fu, H. He, Y. Liu, Q. Wang, L. Xing, X. Xue, Self-powered, stretchable, fiber-based electronic-skin for actively detecting human motion and environmental atmosphere based on a triboelectrification/gas-sensing coupling effect, *J. Mater. Chem. C* 5 (2017) 1231–1239.
- [29] P. Maharjan, R. Toyabur, J. Park, A human locomotion inspired hybrid nanogenerator for wrist-wearable electronic device and sensor applications, *Nano Energy* 46 (2018) 383–395.
- [30] K. Xia, Z. Zhu, H. Zhang, C. Du, Z. Xu, R. Wang, Painting a high-output triboelectric nanogenerator on paper for harvesting energy from human body motion, *Nano Energy* 50 (2018) 571–580.
- [31] Z. Zhang, K. Du, X. Chen, C. Xue, K. Wang, An air-cushion triboelectric nanogenerator integrated with stretchable electrode for human-motion energy harvesting and monitoring, *Nano Energy* 53 (2018) 108–115.
- [32] M. Xu, P. Wang, Y.-C. Wang, S.L. Zhang, A.C. Wang, C. Zhang, Z. Wang, X. Pan, Z. L. Wang, A soft and robust spring based triboelectric nanogenerator for harvesting arbitrary directional vibration energy and self-powered vibration sensing, *Advanced Energy Materials* 8 (2018) 1702432.
- [33] C. He, W. Zhu, B. Chen, L. Xu, T. Jiang, C.B. Han, G.Q. Gu, D. Li, Z.L. Wang, Smart floor with integrated triboelectric nanogenerator as energy harvester and motion sensor, *ACS Appl. Mater. Interfaces* 9 (2017) 26126–26133.
- [34] J. He, T. Wen, S. Qian, Z. Zhang, Z. Tian, J. Zhu, J. Mu, X. Hou, W. Geng, J. Cho, et al., Triboelectric-piezoelectric-electromagnetic hybrid nanogenerator for high-efficient vibration energy harvesting and self-powered wireless monitoring system, *Nano Energy* 43 (2018) 326–339.
- [35] Y. Su, G. Xie, H. Tai, S. Li, B. Yang, S. Wang, Q. Zhang, H. Du, H. Zhang, X. Du, et al., Self-powered room temperature no2 detection driven by triboelectric nanogenerator under uv illumination, *Nano Energy* 47 (2018) 316–324.
- [36] S. Wang, X. Mu, Y. Yang, C. Sun, A.Y. Gu, Z.L. Wang, Flow-driven triboelectric generator for directly powering a wireless sensor node, *Adv. Mater.* 27 (2015) 240–248.
- [37] X. Wang, S. Wang, Y. Yang, Z.L. Wang, Hybridized electromagnetic-triboelectric nanogenerator for scavenging air-flow energy to sustainably power temperature sensors, *ACS Nano* 9 (2015) 4553–4562.
- [38] Y. Yang, G. Zhu, H. Zhang, J. Chen, X. Zhong, Z.-H. Lin, Y. Su, P. Bai, X. Wen, Z. L. Wang, Triboelectric nanogenerator for harvesting wind energy and as self-powered wind vector sensor system, *ACS Nano* 7 (2013) 9461–9468.
- [39] L. Liu, Q. Shi, J.S. Ho, C. Lee, Study of thin film blue energy harvester based on triboelectric nanogenerator and seashore IoT applications, *Nano Energy* (2019) 104167.
- [40] H. Yang, M. Deng, Q. Tang, W. He, C. Hu, Y. Xi, R. Liu, Z.L. Wang, A nonencapsulated pendulum-like paper-based hybrid nanogenerator for energy harvesting, *Adv. Energy Mater.* 9 (2019) 1901149.
- [41] Y. Su, X. Wen, G. Zhu, J. Yang, J. Chen, P. Bai, Z. Wu, Y. Jia, Z.L. Wang, Hybrid triboelectric nanogenerator for harvesting water wave energy and as a self-powered distress signal emitter, *Nano Energy* 9 (2014) 186–195.
- [42] J. Chen, J. Yang, Z. Li, X. Fan, Y. Zi, Q. Jing, H. Guo, Z. Wen, K.C. Pradel, S. Niu, et al., Networks of triboelectric nanogenerators for harvesting water wave energy: a potential approach toward blue energy, *ACS Nano* 9 (2015) 3324–3331.
- [43] X. Fan, J. Chen, J. Yang, P. Bai, Z. Li, Z.L. Wang, Ultrathin, rollable, paper-based triboelectric nanogenerator for acoustic energy harvesting and self-powered sound recording, *ACS Nano* 9 (2015) 4236–4243.
- [44] J. Yang, J. Chen, Y. Liu, W. Yang, Y. Su, Z.L. Wang, Triboelectrification-based organic film nanogenerator for acoustic energy harvesting and self-powered active acoustic sensing, *ACS Nano* 8 (2014) 2649–2657.
- [45] H. Zhao, X. Xiao, P. Xu, T. Zhao, L. Song, X. Pan, J. Mi, M. Xu, Z.L. Wang, Dual-tube helmholtz resonator-based triboelectric nanogenerator for highly efficient harvesting of acoustic energy, *Adv. Energy Mater.* (2019) 1902824.
- [46] S. Li, W. Peng, J. Wang, L. Lin, Y. Zi, G. Zhang, Z.L. Wang, All-elastomer-based triboelectric nanogenerator as a keyboard cover to harvest typing energy, *ACS Nano* 10 (2016) 7973–7981.
- [47] Y. Wang, Y. Yang, Z.L. Wang, Triboelectric nanogenerators as flexible power sources, *Npj Flex. Electron.* 1 (2017) 10.
- [48] J. Chen, H. Guo, G. Liu, X. Wang, Y. Xi, M.S. Javed, C. Hu, A fully-packaged and robust hybridized generator for harvesting vertical rotation energy in broad frequency band and building up self-powered wireless systems, *Nano Energy* 33 (2017) 508–514.
- [49] Q. Tang, M.-H. Yeh, G. Liu, S. Li, J. Chen, Y. Bai, L. Feng, M. Lai, K.-C. Ho, H. Guo, C. Hu, Whirligig-inspired triboelectric nanogenerator with ultrahigh specific output as reliable portable instant power supply for personal health monitoring devices, *Nano Energy* 47 (2018) 74–80.